Journal of Alloys and Compounds 488 (2009) 273–278

Contents lists available at ScienceDirect

Journal of Alloys and Compounds

journal homepage: www.elsevier.com/locate/jallcom

Effects of cathode pulse at low frequency on the structure and composition of plasma electrolytic oxidation ceramic coatings

Zhongping Yao*, Yongjun Xu, Zhaohua Jiang, Fuping Wang

School of Chemical Engineering and Technology, Harbin Institute of Technology, Harbin 150001, PR China

ARTICLE INFO

Article history:
Received 4 August 2009
Received in revised form 18 August 2009
Accepted 22 August 2009
Available online 27 August 2009

Keywords:
Ceramic coatings
Growth characteristic
Plasma electrolytic oxidation
Ti alloy

ABSTRACT

The aim of this work is to investigate the effects of the cathode pulse under the low working frequency on the structure and the composition of the ceramic coatings on Ti–6Al–4V alloys by plasma electrolytic oxidation (PEO). Ceramic coatings were prepared on Ti alloy by pulsed bi-polar plasma electrolytic oxidation in $NaAlO_2$ solution. The phase composition, morphology, and element distribution in the coating were investigated by X-ray diffractometry, scanning electron microscopy, and energy distribution spectroscopy. The coating was mainly composed of a large amount of Al_2TiO_5 and a little α-Al_2O_3 and rutile TiO_2. Increasing the cathode pulse, the amount of rutile TiO_2 was increased while the amount of Al_2O_3 was decreased; and decreasing the cathode pulse, the amount of Al_2O_3 was increased while the amount of rutile TiO_2 was decreased. The thickness of the coatings was increased and then decreased with the increase of the cathode pulse. The grain sizes of Al_2TiO_5 were increased with the cathode current densities, but changed little with the cathode pulse width. The grain size of α-Al_2O_3 was decreased with the decrease of the cathode pulse, while the grain size of TiO_2 was increased with the increase of the cathode pulse. The proper cathode pulse was helpful to reduce the roughness and to increase the density of the coatings.

1. Introduction

Plasma electrolytic oxidation (PEO) technique has been developed rapidly in recent years. The prepared coatings have the fine properties of ceramic coatings like corrosion resistance, anti-abrasion property or decorative property etc. and the promising application prospect in many fields [1–4]. At present, too much research was focused on the composition, the structure and the mechanical properties of the prepared ceramic coatings [5–8]. Although significant progress has been made on the preparation of PEO coatings, the coating formation mechanisms in the PEO process have been least understood yet.

In our previous study, we studied the growth characteristic of the coatings on Ti alloys in $NaAlO_2$ solution by pulsed single-polar PEO power source [9–11]. However, the pulsed bi-polar PEO power source is widely used because of its ability to achieve high quality coatings with large thickness, high micro-hardness, and good adhesion to substrates [12–14]. Generally, the cathode pulse includes two aspects: (1) the cathode current density and (2) the cathode pulse width, which also play important roles in the coating growth. Therefore, the primary objective of this paper was to investigate the effects of cathode pulse current density and cathode pulse width under the low frequency on the growth mechanism of the coatings on Ti–6Al–4V alloys in $NaAlO_2$ solution.

2. Experimental details

2.1. Preparation of plasma electrolytic oxidation ceramic coatings

The present work was conducted on Ti–6Al–4V alloy with a reaction dimension of 25 mm × 15 mm × 6 mm which was used as working electrode. The electrolyser made of stainless steel served as the counter electrode. The electrolytes used in the experiments were Na_2AlO_2 (8 g/L) and Na_3PO_4 (1 g/L). A homemade high power pulsed bi-polar electrical source with power of 10 kW was used for PEO process. The reaction temperature was controlled to below 30 °C by adjusting the cooling water flow. After the PEO treatment, the coated samples were rinsed with water and dried in air.

2.2. Analysis of phase composition and structure of the coatings

Phase composition of the coatings was examined with a RICOH D/max-rB automatic X-ray diffractometer (XRD) using a Cu Kα source. The size of the crystal grain was calculated approximately by Scherrer equation. Surface and section morphology of the coatings was studied by scanning electron microscopy (SEM; Hitachi

* Corresponding author. Tel.: +086 0451 86413710; fax: +086 0451 86415647.
E-mail address: yaozhongping@hit.edu.cn (Z. Yao).

0925-8388/$ – see front matter © 2009 Elsevier B.V. All rights reserved.
doi:10.1016/j.jallcom.2009.08.104

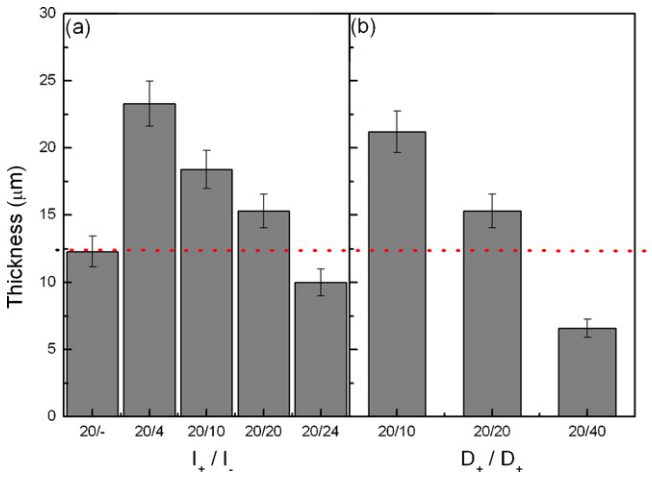

Fig. 1. The thickness of the coatings prepared under different cathode current densities and cathode pulse widths.

S-570). The elemental distribution was investigated by energy dispersive spectroscopy (EDS; US PN5502). The coating thickness was measured, using an eddy current-based thickness gauge (CTG-10, Time Company, China) with a minimum resolution of 1 mm. The average thickness of each sample was obtained from 10 measurements at different positions.

3. Results

3.1. Thickness of the coatings

The thickness of coatings prepared under different cathode pulses is shown in Fig. 1. Panel (a) showed that the coating thickness was increased and then decreased with the increase of cathode current density. When the cathode current density was 4 A/dm^2, the coating thickness was the maximum. Panel (b) showed the thickness of coatings was decreased with the increase of cathode pulse width.

3.2. Composition of the coatings and the sizes of the main crystal grains

Figs. 2 and 3 are the XRD patterns of coatings under different cathode current densities and cathode pulse widths, respectively.

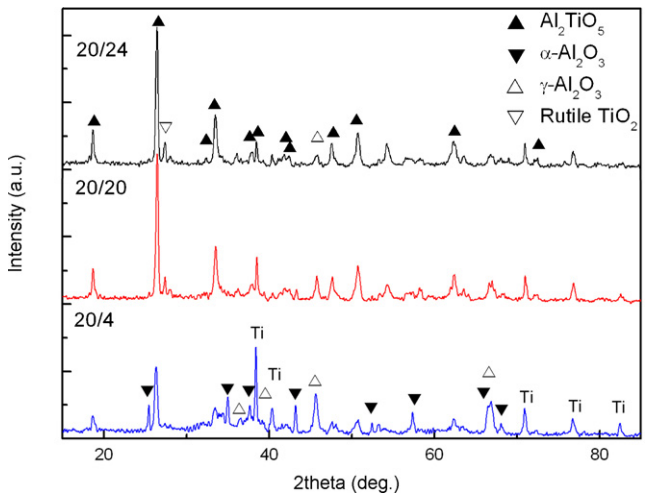

Fig. 2. XRD patterns of the coatings prepared under different cathode current densities (I_+/I_-).

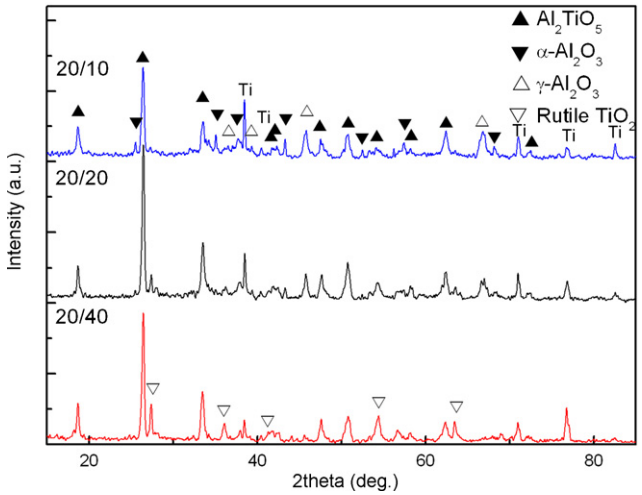

Fig. 3. XRD patterns of the coatings prepared under different cathode pulse widths (D_+/D_-).

Clearly, the coating was mainly composed of a large amount of Al_2TiO_5 and a little Al_2O_3 and rutile TiO_2. Increasing cathode current density, the amounts of Al_2TiO_5 and rutile TiO_2 increased while the amounts of Al_2O_3 decreased. Increasing cathode pulse width, the amount of Al_2TiO_5 firstly increased, and then decreased; and the amount of rutile TiO_2 increased while the amount of Al_2O_3 decreased. Moreover, the diffraction peaks corresponding to Ti were also detected for the coatings, whose intensities reduced with the cathode current densities and the cathode pulse widths although the coating thickness decreased. This illustrates that the density of coatings was improved in a certain degree consequently. The sizes of the crystal grains in the coatings were calculated approximately by Scherrer equation with the results shown in Table 1. The grain sizes of Al_2TiO_5 were increased with cathode current densities, but changed little with cathode pulse width. Also, the grain sizes of α-Al_2O_3 and TiO_2 increased with proper increase of cathode current density or cathode pulse width.

3.3. Surface SEM and the elemental analyses of the coatings

Fig. 4 is the surface SEM of coatings under different cathode pulses. Obviously, there were many sintered particles and many small residual discharging channels. Panels (a and d) show the sintered particles were comparatively large. Increasing cathode current densities (seen in panel b and c) or cathode

Table 1
The size of the crystal grains of the ceramic coatings prepared under different cathode pulses.

	Phases	$2\theta^\circ$	FWHM	Grain size (nm)
I_+/I_- = 20/4	α-Al_2O_3	25.460	0.225	35.79
D_+/D_- = 20/20	Al_2TiO_5	26.360	0.369	21.81
I_+/I_- = 20/20	α-Al_2O_3	25.518	0.185	43.54
D_+/D_- = 20/20	Al_2TiO_5	26.480	0.289	27.93
	TiO_2	27.401	0.341	23.71
I_+/I_- = 20/24	Al_2TiO_5	26.459	0.286	28.22
D_+/D_- = 20/20	TiO_2	27.420	0.255	31.71
I_+/I_- = 20/20	α-Al_2O_3	25.540	0.268	30.06
D_+/D_- = 20/10	Al_2TiO_5	26.440	0.312	25.86
I_+/I_- = 20/20	Al_2TiO_5	26.460	0.300	26.90
D_+/D_- = 20/40	TiO_2	27.400	0.323	25.03

FWHM—Full width at half maximum; I_+—current density of the anode pulse(A/dm^2); I_-—current density of the cathode pulse(A/dm^2); D_+—the duty ratio of the anode pulse(%); D_-—the duty ratio of the cathode pulse(%).

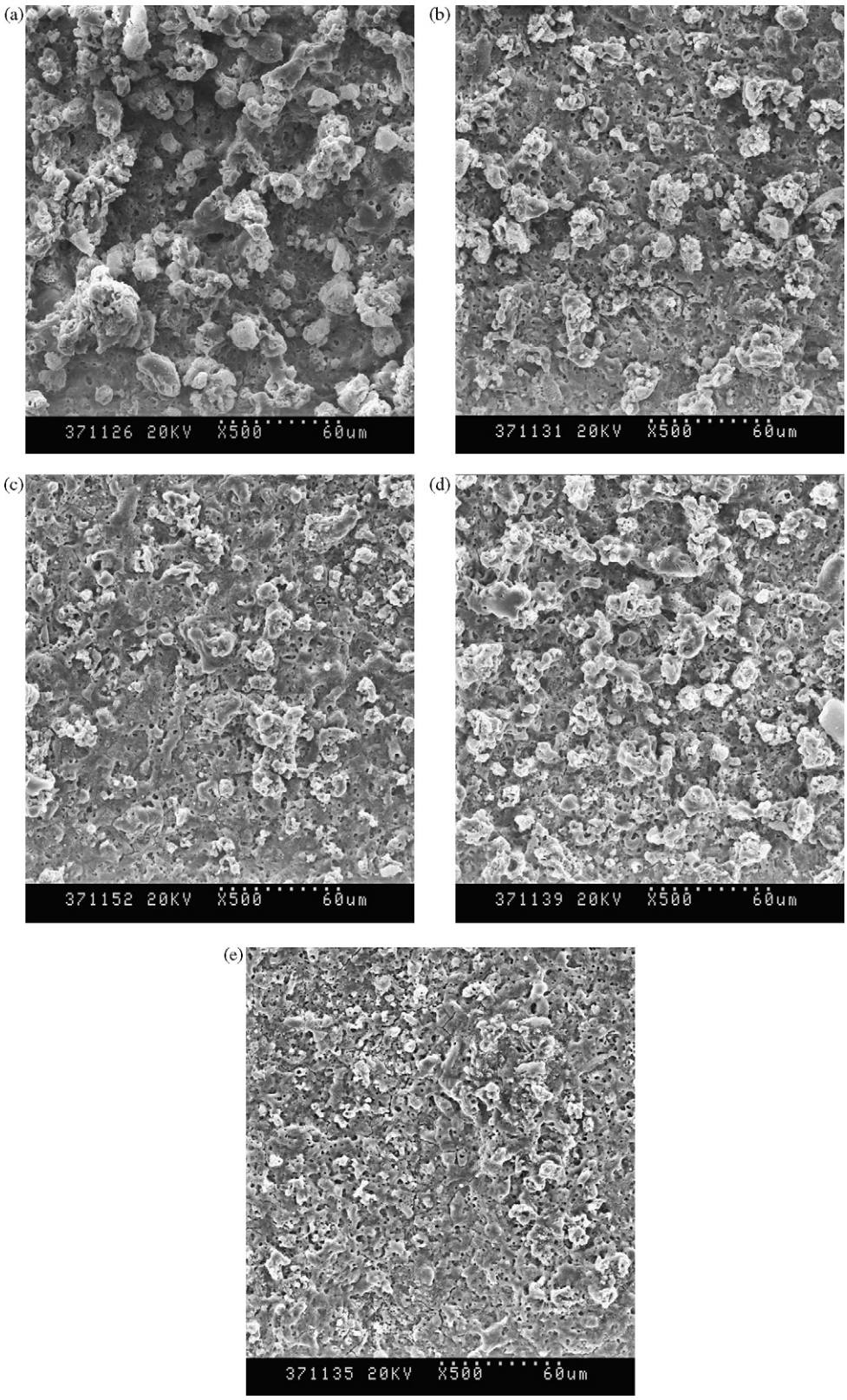

Fig. 4. Surface SEM of the coatings prepared under different cathode current densities and cathode pulse widths. (a): I_+/I_- = 20/4, D_+/D_- = 20/20; (b): I_+/I_- = 20/20, D_+/D_- = 20/20; (c): I_+/I_- = 20/24, D_+/D_- = 20/10; (d): I_+/I_- = 20/20, D_+/D_- = 20/10; (e): $I_+/_-$ = 20/20, D_+/D_- = 20/40.

pulse width (seen in panel b and e), the sintered particles was reduced in both number and size. Table 2 is the EDS analyses on the surface of coatings. Increasing cathode current densities or cathode pulse width, Al content decreased whereas Ti content increased.

3.4. Section SEM and the elemental distribution of the coatings

Fig. 5 is the section SEM of the coatings under different cathode pulses. Increasing the cathode current densities or cathode pulse width, the coating's thickness decreased but the densities

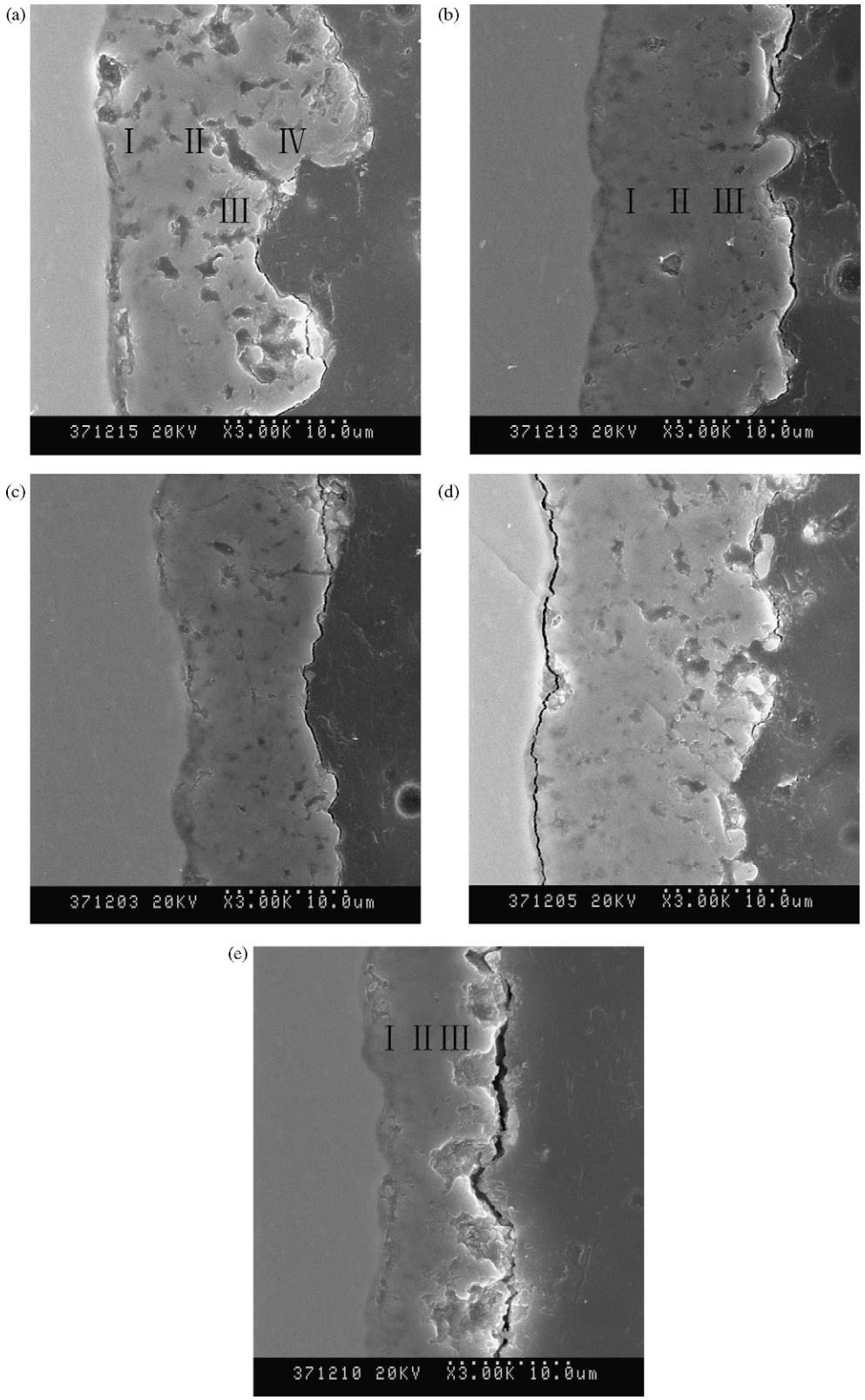

Fig. 5. Section SEM of the coatings prepared under different cathode current densities and cathode pulse widths. I: inner layer; II: middle layer; III and IV: outer layer. (a): I_+/I_- = 20/4, D_+/D_- = 20/20; (b): I_+/I_- = 20/20, D_+/D_- = 20/20; (c): I_+/I_- = 20/24, D_+/D_- = 20/10; (d): I_+/I_- = 20/20, D_+/D_- = 20/10; (e): I_+/I_- = 20/20, D_+/D_- = 20/40.

increased. For panel d, there were apparent gaps between the substrate and the coating (maybe due to the violent shock during the sample cutting and polishing process for the SEM analyses), which showed the bad cohesion between the substrate and the coating. But other panels presented that the coating had good cohesion with the substrate.

In terms of the section images of coatings, the coating was simply divided into three parts, i.e. inner layer, middle layer and outer

Table 2
EDS analyses on the surface of the ceramic coatings prepared under different cathode pulses.

	(a)	(b)	(c)	(d)	(e)
	I_+/I_- = 20/4 D_+/D_- = 20/20	I_+/I_- = 20/20 D_+/D_- = 20/20	I_+/I_- = 20/24 D_+/D_- = 20/20	I_+/I_- = 20/20 D_+/D_- = 20/10	I_+/I_- = 20/20 D_+/D_- = 20/40
Al	55.7	29.7	23.7	36.0	16.7
Ti	44.2	70.3	76.3	64.0	83.3

Table 3
Relative contents (mass%)of the Ti, Al and V in the coatings along the section SEM images in Fig. 5 by EDS analyses.

	(a)				(b)			(d)		
	I_+/I_- = 20/4				I_+/I_- = 20/20			I_+/I_- = 20/20		
	D_+/D_- = 20/20				D_+/D_- = 20/20			D_+/D_- = 20/10		
	I	II	III	IV	I	II	III	I	II	III
Al	14.7	21.7	31.9	54.7	2.0	17.9	57.1	8.9	18.0	23.4
Ti	82.8	75.9	66.3	43.4	94.3	81.3	40.9	86.6	80.0	72.9
V	2.2	2.4	1.9	1.9	3.7	0.8	1.7	4.5	2.0	3.7

layer. The changing trends of the relative amounts of the Ti, Al and V in the coatings are shown in Table 3. All coatings had the similar elemental distribution: Ti content decreased while Al content increased from the interface to the surface. V content in the coating changed little, and was not detected by XRD analyses, which meant that it may be in the form of the amorphous state. For the coating prepared of I_+/I_- = 20/4 and D_+/D_- = 20/20, the amounts of Al and Ti in different positions of the outer layer (seen in III and IV of panel a) were also different. The position far from the inner layer has more Al and less Ti, which was consistent with the diffusion regularity of Ti from the substrate and Al in the electrolyte.

4. Discussion on growth mechanism of PEO coatings

In general, pulsed bi-polar plasma electrolytic oxidation includes an anode pulse and a cathode pulse. During the anode process, a large amount of aluminates ions congregates on the electrode surface due to the effects of the electric field, and an absorption layer of aluminates on the electrode surface was formed, which provided Al joined the PEO reaction. The ceramic coating is generally formed during the anode process. As for the cathode pulse, there are two main effects on the coating forming. One is that the working electrode is under the low potential during the cathode process, which is suitable for the occurrence of some reduction reactions; therefore, it is generally considered that the cathode process probably leads to the dissolution of some oxide phases on the coating surface and therefore, destroys the coating in a certain degree [2]. The other is that the cathode process influences the surface state of the electrode. The absorption layer of aluminates on the electrode takes up the partial working voltage during the anode process. When the cathode pulse is employed, the concentration of aluminates in the absorption layer reduced. This means that the shared voltage of absorption layer decreases and the shared voltage of the working electrode increases under the constant current densities. Compared with the single-polar pulse mode, the more Ti from the substrate dissolves and comes into the coating. In this way the proper cathode pulse is positive to form the coating.

When the small cathode current density or cathode pulse width is applied, the positive effect of the cathode pulse is more than the negative effect, more Ti from the substrate dissolves and the following reactions occurs

$$Ti \rightarrow Ti^{4+} + 4e^- \quad (1)$$

$$Ti^{4+} + 4OH^- \rightarrow TiO_2 + 2H_2O \quad (2)$$

Besides, high-temperature sintering process of aluminates also occurs as follows

$$2Al(OH)^{4-} \rightarrow Al_2O_3 + 2OH^- + 3H_2O \quad (3)$$

Although the amount of dissolved Ti is comparatively increased under this condition, the amount of Al in the absorption layer on the electrode surface is still much more than that of dissolved Ti. This results into the following high-temperature phase transformation.

$$TiO_2(R) + \alpha\text{-}Al_2O_3(\text{at an excess}) \rightarrow Al_2TiO_5{\cdot}Al_2O_3 \quad (4)$$

Therefore, with the increase of cathode pulse, the amount of Al_2TiO_5 is increased while Al_2O_3 exists in the coating and decreases reversely under this condition. And the increase of Al_2TiO_5 is more than the decrease of Al_2O_3, which determines the increase of the thickness of the coating. The grain size of the crystallized substance is determined by the discharging and sintering process. Under the repeating discharging and sintering processes during PEO reaction, the grain size of Al_2TiO_5 increases with the cathode pulse, and the grain sizes of Al_2O_3 also increase although its amount comparatively reduces a little.

Furthermore, the large amount of large sintered particles emerging on the surface of the coating is due to the sintering of the excess Al_2O_3, and therefore, the coating seems rough and coarse. With the increase of the cathode pulse, the sintered particles decreases, which is attributable to the decrease of the amount of Al_2O_3. Consequently, the density of the coatings is also improved.

With the further increase of cathode pulse, whether considering the cathode current density or the cathode pulse width, its destroying effects (reduction) on the coating increases and at the same time the amount of Al in the absorption layer is further decreased while the amount of dissolved Ti from the substrate is comparatively further increased. When the amount of dissolved Ti was more than that of Al in the absorption layer, the following high-temperature phase transformation reaction occurs.

$$\alpha\text{-}Al_2O_3 + TiO_2(R)(\text{at an excess}) \rightarrow Al_2TiO_5{\cdot}TiO_2 \quad (5)$$

Therefore, with the too much increase of the cathode pulse, the amount of Al_2TiO_5 is decreased while TiO_2 exists in the coating and increases reversely under this condition. And the decrease of Al_2TiO_5 is more than the increase of TiO_2, which determines the decrease of the thickness of the coating. The differences of the grain size of Al_2TiO_5 with cathode current density and cathode pulse width show that different degrees of the effects of cathode current density and cathode pulse width on the coating formation. Besides, the grain sizes of TiO_2 increase with the increase of the cathode pulse, which is due to the increase of the amount of TiO_2

in the coating. Because of the further decrease of Al_2O_3 and the increase of TiO_2, the sintered particles emerging on the surface of the coating is small and the coating seems evener and smoother, and meantime the density of the coating is further increased at the cost of the decrease of the thickness of the coating.

Based above analysis, the proper cathode process is liable for the formation of the ceramic coatings and the improvement of the density and smoothness of ceramic coatings. Surely, if the cathode pulse is so strong that the destroying effect of the cathode pulse is more than the coating formation under the anode process, in this way the possible PEO reaction time could be reduced, or even the PEO process could be not occurring at all.

5. Summary

Ceramic coatings on Ti alloy were prepared in $NaAlO_2$ solution by bi-polar pulsed plasma electrolytic oxidation. The effects of the cathode pulse on the structure, composition and growth characteristics of the coatings were investigated and the following conclusions can be drawn:

(1) Compared with the single-polar anode pulse, the thickness of the coatings increased when the small cathode pulse was employed. The further increase of the cathode pulse led to the decrease of the coating thickness, whether considering cathode current density or cathode pulse width. The density and the smoothness of the coating were also increased with the proper increase of the cathode pulse.
(2) The coating was mainly composed of a large amount of Al_2TiO_5 and a little α-Al_2O_3 and rutile TiO_2. Increasing the cathode pulse properly, the amount of Al_2TiO_5 and rutile TiO_2 increased while the amount of Al_2O_3 decreased; and the grain size of the crystallized substances also increased due to the repeating sintering process.

Acknowledgement

This work was financially supported by Special Foundation for New Teachers of Doctor course in Chinese Education Ministry (Grant No. 200802131065).

References

[1] A.L. Yerokhin, X. Nie, A. Leyland, A. Matthews, S.J. Dowey, Surf. Coat. Technol. 122 (1999) 73–93.
[2] A.L. Yerokhin, X. Nie, A. Leyland, A. Matthews, Surf. Coat. Technol. 130 (2000) 195–206.
[3] G. Sundrarajan, L. Rama Krishna, Surf. Coat. Technol. 167 (2003) 269–277.
[4] L.O. Snizhko, A.L. Yerokhin, A. Piikington, N.L. Gurevina, D.O. Misnyankin, A. Leyland, A. Matthews, Electrochim. Acta 49 (2004) 2085–2095.
[5] Y.M. Wang, B.L. Jiang, T.Q. Lei, L.X. Guo, Mater. Lett. 58 (2004) 1907–1977.
[6] W.B. Xue, C. Wang, Y.L. Li, Z.W. Deng, R.Y. Chen, T.H. Zhang, Mater. Lett. 56 (2002) 737–743.
[7] H. Habazaki, M. Uozumi, H. Konno, K. Shimizu, P. Skeldon, G.E. Thompson, Corros. Sci. 45 (2003) 2063–2073.
[8] X. Nie, E.I. Meletis, J.C. Jiang, A. Leyland, A.L. Yerokhin, A. Matthews, Surf. Coat. Technol. 149 (2002) 245–251.
[9] Z.P. Yao, R.H. Cui, Z.H. Jiang, F.P. Wang, Appl. Surf. Sci. 253 (2007) 6778–6783.
[10] Z.P. Yao, Y.L. Jiang, Z.H. Jiang, F.P. Wang, J. Mater. Sci. 42 (2007) 9434–9439.
[11] Z.P. Yao, Y.L. Jiang, F.Z. Jia, Z.H. Jiang, F. P. Wang, Appl. Surf. Sci. 254 (2008) 4084–4091.
[12] Y. Hirata, M. Fukushima, T. Sano, K. Ozaki, T. Ohji, Vacuum 59 (2000) 142–151.
[13] F. Schlottig, J. Schreckenbach, D. Dietrich, A. Hofmann, G. Marx, Appl. Surf. Sci. 90 (1995) 129–136.
[14] H. Kawamura, K. Moritani, Y. Ito, Plasmas Ions 1 (1998) 29–36.